

## Coherently coupled ZnO and VO<sub>2</sub> interface studied by photoluminescence and electrical transport across a phase transition

Amar Srivastava, T. S. Heng, Surajit Saha, Bao Nina, A. Annadi, N. Naomi, Z. Q. Liu, S. Dhar, Ariando, J. Ding, and T. Venkatesan

Citation: *Applied Physics Letters* **100**, 241907 (2012); doi: 10.1063/1.4729387

View online: <http://dx.doi.org/10.1063/1.4729387>

View Table of Contents: <http://scitation.aip.org/content/aip/journal/apl/100/24?ver=pdfcov>

Published by the AIP Publishing

---

### Articles you may be interested in

[Role of defect states in magnetic and electrical properties of ZnO nanowires](#)

*AIP Advances* **3**, 042110 (2013); 10.1063/1.4801937

[Electric field induced reversible control of visible photoluminescence from ZnO nanoparticles](#)

*Appl. Phys. Lett.* **98**, 153109 (2011); 10.1063/1.3578194

[Polarity-related asymmetry at ZnO surfaces and metal interfaces](#)

*J. Vac. Sci. Technol. B* **27**, 1710 (2009); 10.1116/1.3119681

[Photoluminescence and polarized photodetection of single ZnO nanowires](#)

*Appl. Phys. Lett.* **85**, 6128 (2004); 10.1063/1.1841453

[Photoluminescence dependence of ZnO films grown on Si\(100\) by radio-frequency magnetron sputtering on the growth ambient](#)

*Appl. Phys. Lett.* **82**, 2625 (2003); 10.1063/1.1568543

---



## Coherently coupled ZnO and VO<sub>2</sub> interface studied by photoluminescence and electrical transport across a phase transition

Amar Srivastava,<sup>1,2</sup> T. S. Heng,<sup>3</sup> Surajit Saha,<sup>1,2</sup> Bao Nina,<sup>1</sup> A. Annadi,<sup>1,2</sup> N. Naomi,<sup>1,2</sup> Z. Q. Liu,<sup>1,2</sup> S. Dhar,<sup>1,4</sup> Ariando,<sup>1,2</sup> J. Ding,<sup>1,3</sup> and T. Venkatesan<sup>1,2,4,a)</sup>

<sup>1</sup>NUSNNI-NanoCore, National University of Singapore, Singapore 117576

<sup>2</sup>Department of Physics, National University of Singapore, Singapore 117542

<sup>3</sup>Department of Materials Science and Engineering, National University of Singapore, Singapore 119260

<sup>4</sup>Department of Electrical and Computer Engineering, National University of Singapore, Singapore 117576

(Received 21 May 2012; accepted 25 May 2012; published online 15 June 2012)

We have investigated the photoluminescence and electrical properties of a coherently coupled interface consisting of a ZnO layer grown on top of an oriented VO<sub>2</sub> layer on sapphire across the phase transition of VO<sub>2</sub>. The band edge and defect luminescence of the ZnO overlayer exhibit hysteresis in opposite directions induced by the phase transition of VO<sub>2</sub>. Concomitantly the phase transition of VO<sub>2</sub> was seen to induce defects in the ZnO layer. Such coherently coupled interfaces could be of use in characterizing the stability of a variety of interfaces *in situ* and also for novel device application. © 2012 American Institute of Physics. [<http://dx.doi.org/10.1063/1.4729387>]

Among the many transition metal oxides that exhibit metal to insulator transition (MIT) (which can be induced by temperature, stress or doping), vanadium oxide (VO<sub>2</sub>) has been studied intensely on account of the closeness of its MIT to room temperature and also for its potential application as field effect switches, optical detectors, nonlinear circuit components, and solid-state sensors.<sup>1-4</sup> Vanadium oxide (VO<sub>2</sub>) undergoes MIT (Ref. 5) at  $T_{MIT} = 341$  K accompanied by a structural phase transition (SPT) from a room-temperature monoclinic phase to a high-temperature tetragonal phase at and beyond  $T_{MIT}$ . (In this paper, the SPT and MIT are used interchangeably). The phase transition is also accompanied by strong changes in the dielectric constant with high transparency in the semiconductor phase and high reflectivity in the metallic phase in a broad frequency spectrum including the telecommunications window with a hysteresis in optical transmittance.<sup>6,7</sup> SPT can be understood as a change in crystal lattice symmetry associated with the tilting of VO<sub>6</sub> octahedron and dimerization of vanadium atoms along the *c*-axis which causes a 0.6% contraction along the  $a_t$  (*a*-axis of the tetragonal phase), 0.4% contraction along  $b_t$  (*b*-axis) while along  $c_t$  (*c*-axis), it gets elongated by 1.0% for the transition to monoclinic phase.<sup>8</sup> Taking advantage of the spontaneous strain associated with the phase transition, a colossal thermo-mechanical actuation in VO<sub>2</sub> micro-cantilevers was reported, making them suitable for thermal sensors, energy transducers, and actuators with unprecedented sensitivities.<sup>9</sup> Thus the phase transition of VO<sub>2</sub> can be utilized to exert a large strain on an over-layer across the MIT. If the (VO<sub>2</sub>) phase transition can induce a strain on the over layer and change its optical or magnetic property then the phase transition can be monitored by other than transport measurement which will give an extra degree of freedom in device design. On the other hand, such strain can also induce defects in the over layer which could also be monitored by measuring the over layer property leading to a better understanding of the behavior of materials under stress.

There are very few reports on how the strain induced by the phase transition of VO<sub>2</sub> affects the properties of an over-layer. ZnO, the over layer used in this study, is recognized as a key material with a wide variety of commercial applications due to its outstanding versatility in electrical, optical, and chemical properties. In this study, we use the MIT in VO<sub>2</sub> to induce a significant strain on the ZnO over layer and by studying the photoluminescence (PL) of the ZnO layer try to understand the response of the defects in the ZnO film to this *in-situ* strain. Since the PL signals of ZnO arising from band edge and defects are well understood, this will constitute an ideal coherently coupled interface that can be monitored across an MIT. This may pave the way for the study of the structural stability of a variety of interfaces.

VO<sub>2</sub> films were grown using pulsed laser deposition (PLD) technique. Commercially available single crystal target of vanadium metal (99.99% pure) was used for the deposition. VO<sub>2</sub> films were deposited at optimized pressure and temperature of 10<sup>-3</sup> Torr and 500 °C, respectively, as reported elsewhere.<sup>10</sup> Single crystal ZnO (99.99% pure) target was used for the deposition of 100 nm thick ZnO films (as confirmed by Rutherford back scattering (RBS) spectrometry) at a temperature of 350 °C in order to avoid the formation of different phases of VO<sub>2</sub> when exposed to high temperature. Followed by the deposition of ZnO, the bilayer was annealed in oxygen at a pressure of 10<sup>-3</sup> Torr and 600 °C to improve the quality of both the VO<sub>2</sub> and ZnO layers. Growth and orientation of the films were examined using x-ray diffraction (Bruker D8 Discover). The photoluminescence measurements were performed (iHR 550 spectrometer) using a 325 nm line from a He-Cd laser as the excitation source and the sample temperature was varied with a Janis closed-cycle helium cryostat system in the temperature ranges of 10-400 K. The electrical transport measurements were performed with van der Pauw geometry (Quantum Design-PPMS).

PLD deposited films on *c*-axis sapphire showed high quality growth of VO<sub>2</sub> and ZnO as seen by the  $\theta$ - $2\theta$  (Fig. 1(a), (i)) which show predominantly (020) VO<sub>2</sub> and (0002) ZnO on VO<sub>2</sub>/Al<sub>2</sub>O<sub>3</sub>. The phi scans of the ZnO (10 $\bar{1}$ 1)

<sup>a)</sup> Author to whom correspondence should be addressed. Electronic mail: venky@nus.edu.sg. Tel.: +65-65165187. Fax: +65-68725563.

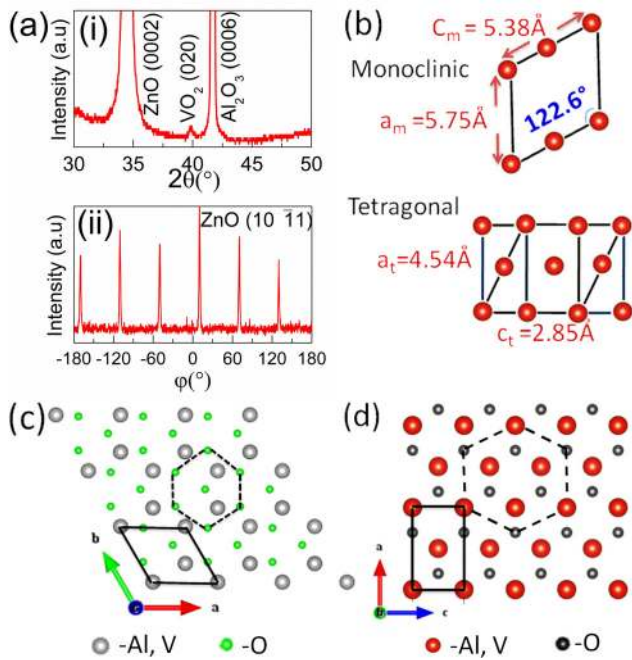


FIG. 1. (a), (i)  $\theta$ - $2\theta$  scan of the ZnO on  $\text{VO}_2/\text{Al}_2\text{O}_3$ , (ii) Phi scan of the ZnO overlayer, (b) A model for monoclinic and tetragonal  $\text{VO}_2$  phase by slight displacement of vanadium atoms. (c) Position of vanadium atoms in the unit cell of epitaxially grown (020)  $\text{VO}_2$  thin films on  $\text{Al}_2\text{O}_3$  (0006) and (d) schematic of orientation of (0002) ZnO plane on (020)  $\text{VO}_2$ .

plane shown in (Fig. 1(a), (ii)). The phi-scan peaks at  $60^\circ$  intervals are consistent with the hexagonal symmetry of the epitaxial ZnO wurtzite structure. Fig. 1(b) shows schematic<sup>11</sup> location and displacement of V atoms during the phase transition from monoclinic to tetragonal across the metal insulator transition temperature. Figs. 1(c) and 1(d) show position of vanadium atoms in the unit cell of epitaxially grown (020)  $\text{VO}_2$  thin films on  $\text{Al}_2\text{O}_3$  (0006) and a schematic of the orientation of (0002) ZnO plane on (020)  $\text{VO}_2$ , respectively. Since the  $\text{VO}_2$  grows with the “a” and “c” in plane, the ZnO is subjected to lattice strain along both these directions. The estimated tensile strain in ZnO along the “ $c_t$ ” axis is  $\sim 1\%$  and  $0.6\%$  along the “ $a_t$ ” direction at and above the MIT.

Fig. 2(a) shows a typical resistivity vs. temperature behavior of  $\text{VO}_2$  films grown on  $c$ -axis  $\text{Al}_2\text{O}_3$ . The resistivity shows a drop of 4 orders of magnitude across the MIT (341 K) with a hysteresis width of 12 K. We have measured the resistivity of the ZnO- $\text{VO}_2$  over layer and observed a hysteresis that is broader in the as-deposited ZnO film on  $\text{VO}_2$  with a smaller resistivity change (Fig. 2(b)). This is mainly due to the capping action of the ZnO which changes

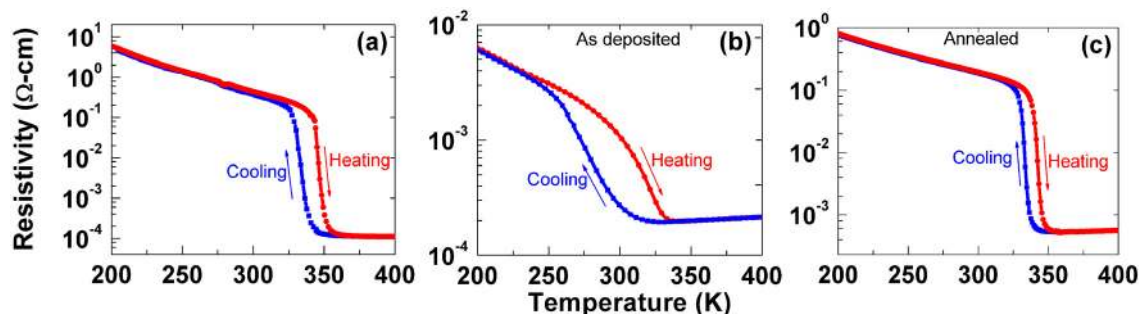


FIG. 2. Resistance versus temperature of the (a)  $\text{VO}_2$  layer prior to the ZnO deposition. (b) As deposited ZnO/ $\text{VO}_2$ / $\text{Al}_2\text{O}_3$ . (c) Annealed at  $10^{-3}$  Torr,  $600^\circ\text{C}$ .

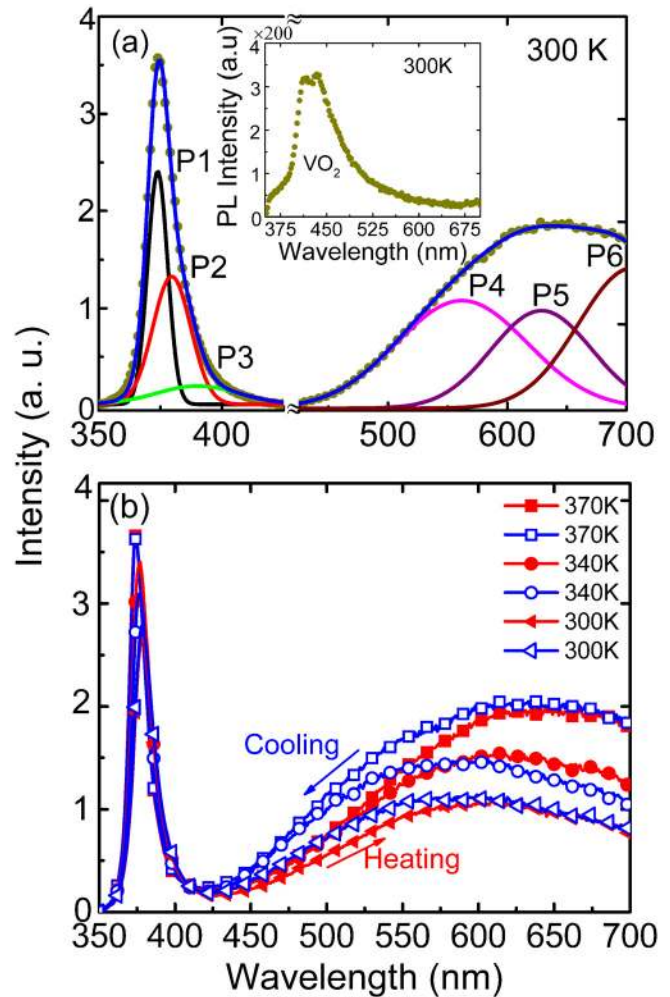


FIG. 3. (a) Photoluminescence data of band edge emission ( $<425\text{ nm}$ ), defect band emission ( $>425\text{ nm}$ ) and its Gaussian fitting for ZnO/ $\text{VO}_2$ / $\text{Al}_2\text{O}_3$ . The inset shows the photoluminescence of  $\text{VO}_2/\text{Al}_2\text{O}_3$  at 300 K. (b) PL Intensity at three different temperatures 300 K, 340 K, 370 K during heating and cooling for ZnO/ $\text{VO}_2$ / $\text{Al}_2\text{O}_3$ .

the oxygen stoichiometry of the  $\text{VO}_2$  layer. The actual width of hysteresis of the transition of  $\text{VO}_2$  is more than recovered ( $\sim 7\text{ K}$ ) upon annealing in oxygen ambience at  $10^{-3}$  Torr and  $600^\circ\text{C}$ . The dynamic range of the resistivity spans a smaller range compared to the  $\text{VO}_2$  alone due to the shunting effect of the ZnO conductivity. The hysteretic behavior of MIT in  $\text{VO}_2$  remains intact despite the fact that a 100 nm thick ZnO film is on top.

In Fig. 3(a) is shown the PL signal from the ZnO film on  $\text{VO}_2$  subsequent to annealing in oxygen ambience at  $600^\circ\text{C}$ .

In the high energy side, as shown in Fig. 3(a), the band edge luminescence can be fitted by three components centered at, 373.96 nm (3.32 eV), 379.67 nm (3.26 eV), and 390.07 nm (3.18 eV). The peak at 3.32 eV can be assigned to a donor–acceptor pair transition<sup>12</sup> and those at 3.26 eV and 3.18 eV can be assigned to phonon replicas of the 3.32 eV peak. On the low-energy side of the PL spectrum at 300 K (Fig. 3(a)), the peaks at 560.45 nm (2.2 eV) (yellow band), 613.34 nm (2.02 eV) (orange band), and 678.3 nm (1.83 eV) (red band) can be assigned to three deep-level emissions arising from defects. The peak at 1.83 eV can be attributed to a donor–acceptor–pair transition with the acceptor being a Zn vacancy ( $V_{Zn}$ ) consistent with the literature reports, while the 2.2 and 2.02 eV (yellow/orange) emission peaks are associated with oxygen interstitials ( $O_i$ ).<sup>13–15</sup> Another interesting observation is the lack of a large green band (2.45 eV) in our ZnO films which is usually the dominant deep level feature in ZnO seen in the spectra of bulk crystals.<sup>16</sup> The strong red band (1.83 eV indicating the presence of Zn vacancies) and lack of the green band (absence of O vacancies) in our thin films suggest an O-rich growth condition. For comparison, we have also recorded the PL spectrum of  $VO_2$  thin film which is shown in the inset of Fig. 3(a). It can be seen that the intensity of PL signal of  $VO_2$  is very weak compared to that of ZnO which infers that the PL signal of ZnO, as shown in Fig. 3(a), has negligibly small contribution from  $VO_2$ .

Fig. 3(b) shows the results of PL measurements at three different temperatures, at 300 K (insulating region of  $VO_2$ ), around MIT of  $VO_2$  at 340 K and at 370 K well above the MIT (metallic region of  $VO_2$ ) during the heating and cooling cycles. A clear hysteresis is seen in the defect emission and also the band edge emission. The band edge luminescence

(integrated over 350–425 nm) and the defect luminescence (integrated over 425–650 nm) are plotted as a function of temperature in Figs. 4(a)–4(d) for different thermal cycles. The integrated PL intensity of the band edge and defect peaks of single crystal ZnO as shown in the inset of Figs. 4(c) and 4(d) shows a typical temperature-dependent PL, i.e., a monotonic decrease in PL intensity with increasing temperature, due to the increased non-radiative recombination.

However, the ZnO over-layer on  $VO_2$  (Fig. 4(a)) shows an increase in the PL intensity while heating till the MIT (the origin of which is not understood) followed by a dramatic drop in the intensity which remains low upon cooling back to 300 K. This hysteresis is much broader than the electrical hysteresis shown in Fig. 2(c) which was actually measured during the second thermal cycle. These data clearly indicate the formation of defects in ZnO which do not recover when the  $VO_2$  recovers its original phase electrically.

This is further supported by the defect luminescence in Fig. 4(b) which also shows a broad hysteresis curve excepting that there is a decrease while heating and an increase while cooling (opposite to the behavior of the band edge luminescence) implying an accumulation of defects in the ZnO due to the MIT of  $VO_2$ . After a few thermal cycles, the hysteresis curves for both the band edge and the defect luminescence become narrow as shown in Figs. 4(c) and 4(d). If one looks at the changes in the defect luminescence, the predominant changes are found to occur at 2.02 and 2.2 eV transitions which are related to oxygen interstitials. This suggests that when the ZnO layer is subjected to the  $\sim 1\%$  strain at the  $VO_2$  interface, the film responds by creating oxygen interstitials to accommodate the strain. When the  $VO_2$  layer recovers, the oxygen interstitials do not recombine concomitantly

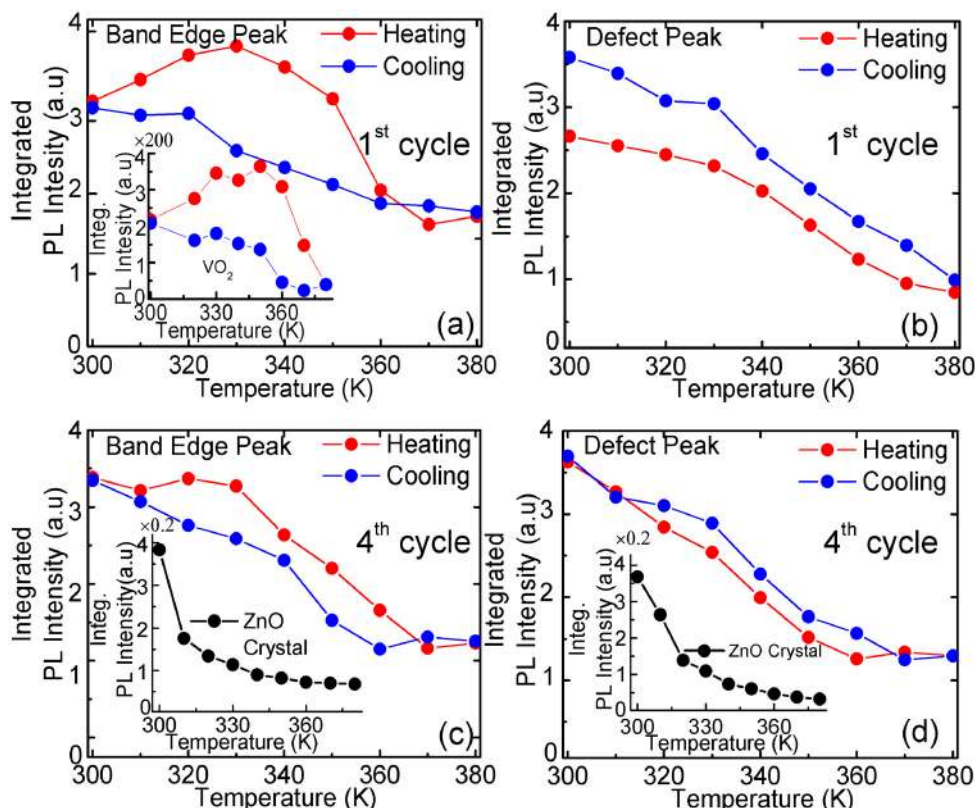


FIG. 4. Effect of heat cycling for (a), (c) band edge peak (integrated over 350–425 nm). (b), (d) Defect peak (integrated over 425–650 nm) after 1st and 4th heat cycle, respectively, from annealed ZnO/ $VO_2$ / $Al_2O_3$ . The inset of (a) shows the PL from  $VO_2$  (integrated between 350 and 425 nm). The inset of (c) and (d) shows the band edge (integrated over 350–425 nm) and defect peak (integrated over 425–650 nm) of ZnO single crystal, respectively.

leaving a defective ZnO over a larger temperature range. It is highly likely that under such strain the ZnO layer may also form some dislocations. When such dislocations form, under subsequent cycles, part of the strain will be accommodated by the dislocations and hence less oxygen interstitials need to be created which reduces the difference between the heating and cooling cycles narrowing the hysteresis curves. In a recent paper on VO<sub>2</sub> nanoparticles embedded with gold,<sup>17</sup> a large optical transmission hysteresis was shown. However, in this case, the electrical hysteresis could not be measured. So in this case, the broad optical hysteresis could be associated with material inhomogeneity. Moreover, Raman spectroscopy by Donev *et al.*<sup>18</sup> shows a broader hysteresis in smaller nanostructures of VO<sub>2</sub> compared to that in thin films thus attributing it to the defects. Therefore, in our experiment, the broadening of the PL hysteresis is a sure indicator of defect formation. Interestingly, the PL intensity of VO<sub>2</sub> (integrated between 350 and 425 nm) shows a broad hysteresis much like the case of ZnO (shown in the inset of Fig. 4(a)). This indicates the presence of defects in VO<sub>2</sub> which do not show up in electrical measurements but are very visible in the optical measurements.

In conclusion, the coherently coupled interfaces of ZnO and VO<sub>2</sub> enable us to probe the stability of the ZnO at the interface when subjected to the strain under a SPT. The photoluminescence in the ZnO layer enables us to understand the response of the ZnO to this strain and even help identify the specific defects that are manifested to counter the strain. Such coherently coupled interfaces where a strong SPT in one layer can be parlayed to an over-layer may enable us to design variety of devices and in addition serve as an *in-situ* tool to study the effect of interface strain on the stability of various over layers.

We acknowledge the NUSNNI-NanoCore at the National University of Singapore, Singapore for the support. We would like to acknowledge for financial support from NRF-CRP “Tailoring Oxide Electronics by Atomic Control” Grant No. NRF2008NRFCRP002-024, NUS YIA, NUS cross-faculty grant, FRC, and BMBF.

- <sup>1</sup>D. M. Newns, T. Doderer, C. C. Tsuei, W. M. Donath, J. A. Misewich, A. Gupta, B. M. Grossman, A. Schrott, B. A. Scott, P. C. Pattnaik, R. J. von Gutfeld, and J. Z. Sun, *J. Electroceram.* **4**, 339 (2000).
- <sup>2</sup>C. E. Lee, R. A. Atkins, W. N. Gibler, and H. F. Taylor, *Appl. Opt.* **28**, 4511 (1989).
- <sup>3</sup>Y. Wook Lee, B.-J. Kim, S. Choi, H.-T. Kim, and G. Kim, *Opt. Express* **15**, 12108 (2007).
- <sup>4</sup>M. A. Richardson and J. A. Coath, *Opt. Laser Technol.* **30**, 137 (1998).
- <sup>5</sup>S. Hormoz and S. Ramanathan, *Solid-State Electron.* **54**, 654 (2010).
- <sup>6</sup>J. B. Kana Kana, J. M. Ndjaka, B. D. Ngom, N. Manyala, O. Nemraoui, A. Y. Fasasi, R. Nemitudi, A. Gibaud, D. Knoesen, and M. Maaza, *Thin Solid Films* **518**, 1641 (2010).
- <sup>7</sup>H. W. Verleur, A. S. Barker, Jr., and C. N. Berglund, *Phys. Rev.* **172**, 788 (1968).
- <sup>8</sup>A. Tselev, V. Meunier, E. Strelcov, W. A. Shelton, I. A. Luk'yanchuk, K. Jones, R. Proksch, A. Kolmakov, and S. V. Kalinin, *ACS Nano* **4**, 4412 (2010).
- <sup>9</sup>J. Cao, W. Fan, H. Zheng, and J. Wu, *Nano Lett.* **9**, 4001 (2009).
- <sup>10</sup>D. Ruzmetov, S. D. Senanayake, V. Narayanamurti, and S. Ramanathan, *Phys. Rev. B* **77**, 195442 (2008).
- <sup>11</sup>K. Okimura, *J. Appl. Phys.* **107**, 063503 (2010).
- <sup>12</sup>S. Chooapun, R. D. Vispute, W. Noch, A. Balsamo, R. P. Sharma, T. Venkatesan, A. Iliadis, and D. C. Look, *Appl. Phys. Lett.* **75**, 3947 (1999).
- <sup>13</sup>C. V. Manzano, D. Alegre, O. Caballero-Calero, B. Alen, and M. S. Martin-Gonzalez, *J. Appl. Phys.* **110**, 043538 (2011).
- <sup>14</sup>B. Lin, Z. Fu, and Y. Jia, *Appl. Phys. Lett.* **79**, 943 (2001).
- <sup>15</sup>L. E. Greene, M. Law, J. Goldberger, F. Kim, J. C. Johnson, Y. Zhang, R. J. Saykally, and P. Yang, *Angew. Chem., Int. Ed.* **42**, 3031 (2003).
- <sup>16</sup>F. Wen, W. Li, J.-H. Moon, and J. Hyeok Kim, *Solid State Commun.* **135**, 34 (2005).
- <sup>17</sup>E. U. Donev, J. I. Ziegler, J. R. F. Haglund, and L. C. Feldman, *J. Opt. A, Pure Appl. Opt.* **11**, 125002 (2009).
- <sup>18</sup>E. U. Donev, R. Lopez, L. C. Feldman, and R. F. Haglund, *Nano Lett.* **9**, 702 (2009).